2015

The Numerical Solution of the Exterior Impedance (Robin) Problem for the Helmholtz's Equation via Modified Galerkin Method: Superllipsoid

Hy Dinh
Roger Williams University, hdinh885@g.rwu.edu

The Numerical Solution of the Exterior Impedance (Robin) Problem for the Helmholtz's Equation via Modified Galerkin Method: Superellipsoid

Hy Dinh
Advisor: Dr. Yajni Warnapala

Dept. of Mathematics
Roger Williams University

May 2015

This thesis is dedicated to my parents, Quy Dinh and Hien Ngo, and my advisor, Dr. Warnapala.

Abstract

This thesis focuses on finding the solution for the exterior Robin Problem for the Helmholtz Equation and therefore, determines how a convergent smooth surface depending on its outer shape, in this case the superellipsoid, responds to different outer waves. The primary purpose is to calculate the possibility of a certain object, acquiring sufficient conditions, to either submerge under respectively high water pressure or maintain in outer space; if applicable, this approach can be used for a new efficient design of a portion of a submarine or part of a space craft, the second of more interest to NASA, one of my sponsors. In this thesis, I analyze the numerical solution for the Helmholtz equation in 3 Dimensions, for the superellipsoid for the Robin Boundary Condition and answer the question of how a surface reacts to incoming waves approaching from various directions. Would the object tend to the extremes of either absorbing or reflecting everything with which it comes into contact, or would it obtain a neutral combination of the two.

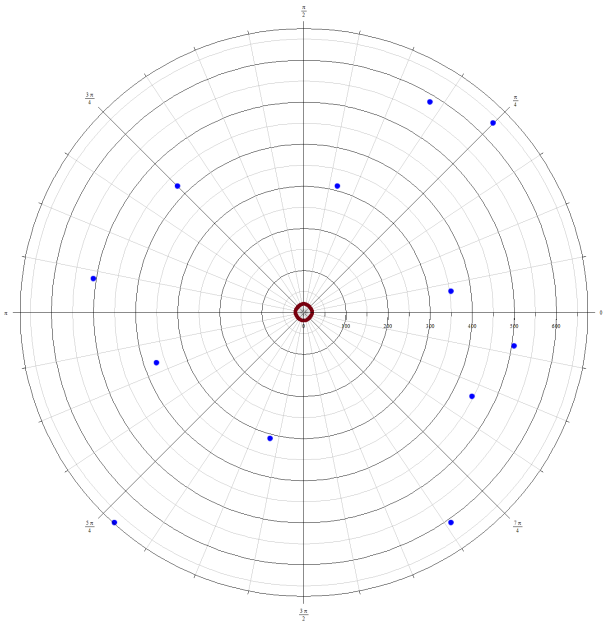

(This diagram shows the general interpretation of the research. The red circle represents the superellipsoid and the blue dots are point source where the waves originated from.)

1 Introduction

The Helmholtz Equation, also known as the wave equation, emerges when the topic of electromagnetism and radiation are discussed. It consists of a combination of partial differential equations that models how a previously defined object reacts towards waves coming from arbitrary direction.

In reality, most surrounding objects are exposed to various types of waves. However, the reactions are neglected for being insignificant and also not observable by the naked eye. In this thesis, I will focus on the acoustic aspects of the Helmholtz Equation when the object is submerged underwater or located in the outer space. The surface defined by the object should be smooth and simply connected. I applied the Green's Functions approach by reducing the problem to a boundary value problem by disregarding what happens in the interior of the desired object and only looking at its boundary. In previous papers, the Neumann and Dirichlet conditions were analyzed. However, they only study the two extremes of reflecting (Neumann) and absorbing (Dirichlet) the waves that come in contact with the surface. I investigated the more realistic condition that combines the previous two conditions, the Impedance (Robin) condition.

The Helmholtz Equation was solved analytically via separation of variables for the circular membrane by Alfred Clebsch [7] and for the elliptical membrane by Emile Mathieu [3] under the condition that the wave particles move in predictable straight lines. There is no exact solution for the wave equation if the movement is more complicated. Therefore, the solutions are often approximated through numerical methods. The first step for any numerical method is to discretize the problem; the common techniques are finite difference methods – for simple shapes, and finite element methods – for more complicated geometries [13]. They share the general idea of dividing the object into smaller sub-regions. Thus I utilized the Modified Galerkin Method, finite element method for multi-dimensional space with non-congruent grids. However, since the fundamental solution, $\frac{e^{ikr_{qA}}}{r_{qA}}$ has a weak singularity at points near the boundary, I enhanced the method by adding an infinite series to reduce the discontinuity effects. The object I considered was the superellipsoid, modeled by the following equations:

$$\begin{aligned} x &= \cos(\alpha)\sin^n(\beta) \qquad & n &\in [0.5, 5] \\ y &= \sin(\alpha)\sin^n(\beta) \qquad & \alpha &\in [-\pi, \pi] \\ z &= \cos(\beta) \qquad & \beta &\in [-\pi, \pi] \end{aligned}$$

The cross sectional superellipsoidal shape varies from a pinched-in diamond to a diamond and expands towards a square-like shape. All of these deviations can be obtained by changing the n-value (a sphere has n = 1 and the smaller n becomes, the closer to a square the cross sectional shape gets). I limited the range of the superellipsoid so that it does not have any sharp edges and is not a perfect sphere, for the sphere was already studied in a previous paper [10]. Some representatives of the superellipsoid are shown below with different n values. I primarily concentrated on the shape with n = 1.4 since it has a smooth and continuous surface and also provides the best convergence results compared to shapes with similar n values.

Note: Similar experiments were conducted for the following shapes: sphere, ellipsoid, oval of Cassini, and pseudosphere [8, 9, 10]

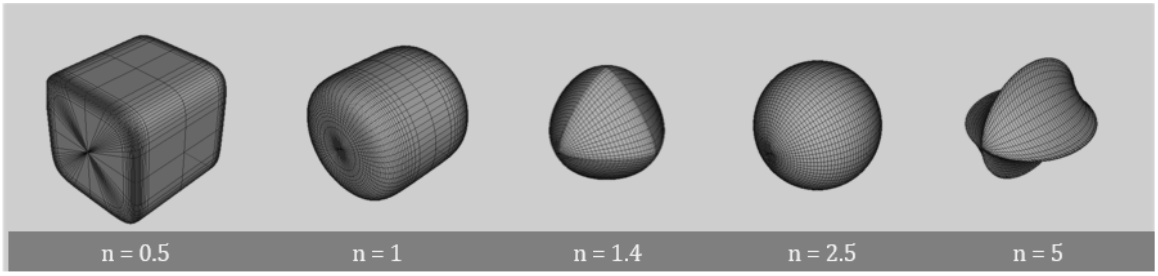

Figure 1: Supersllipsoid shape

2 Preliminary Definition

2.1 The Helmholtz Equation

The research revolves around applications of the Helmholtz Equation, studying how an object, with appropriate initial conditions reacts towards incoming waves from arbitrary directions. The general form of the equation is

$$\Delta u(A) + k^2 u(A) = 0 \qquad Im\ k \geq 0, \text{where k is the wave number}$$
$$\Delta = \frac{\partial^2}{\partial x^2} + \frac{\partial^2}{\partial y^2} + \frac{\partial^2}{\partial z^2}$$

A is an arbitrary point located exterior to the object.

2.2 The Impedance (Robin) Condition

For this research project, I investigated the case where the waves are partially deflected and partially absorbed by the boundary of the object. In other words, the Impedance (Robin) condition was applied. Let S be a closed bounded surface in $\Re^3$, andD_+ the exterior domain of S [9], then the boundary condition satisfied

$$\lambda u(p) + \frac{\partial u(p)}{\partial v_p} = f(p)$$

where f and u are given continuous functions on ∂D and λ the coefficient for the weight of absorption and reflection. For the purpose of this research, I assumed a 1:1 ratio ($\lambda = 1$). This ratio is a combination of the geometry, material of the object and how the object is manufactured. Therefore, by specifying a certain material, λ can be further adjusted to accommodate the problem. Here, u satisfies the Sommerfeld radiation condition which indicates that a point source radiates waves toward the object in order to focus on the waves coming from outside of the object [9].

2.3 Spherical Harmonics

The angular portion of the solution for Laplace's equation in spherical coordinates are written in terms of the spherical harmonic functions, $\Upsilon_t^m(\theta, \phi)$. They form an orthogonal system and are used in application involving gravitational fields and magnetic fields [10].

2.4 Fredholm Integral Equations

Fredholm Integral Equations are crucial for understanding and applying spectral theory which concerns itself with finding eigenvectors and eigenvalues of a desired matrix. In this thesis, I used the Fredholm Equation of second kind, in which the general form is shown below.

$$u(t) = f(t) + \lambda \int_a^b K(t,s)\phi(s)ds$$

The kernel $K(t,s)$ and the function $f(t)$ are given functions [8].

2.5 Green's Theorem

The Green's Theorem approach reduces a problem by neglecting the interior of an object but only analyzing the integral on the boundary. Given a smooth and simply connected region R, the double integral over R can be transformed to a line integral over the boundary of R. [8]

$$\iint_R \left(\frac{\partial Q}{\partial x} - \frac{\partial P}{\partial y}\right) dA = \oint_{\partial R} (Pdx + Qdy)$$

2.6 Volume of a superellipsoid

The volume of a superellipsoid can be calculated via the following formula

$$V(r,n) = 8r^3 \frac{\left[\Gamma\left(1+\frac{1}{n}\right)\right]^3}{\Gamma\left(1+\frac{3}{n}\right)}$$

where r and n are the radius and n-value of the specific superellipsoid respectively. There is no closed form for the surface area of the superellipsoid

2.7 Integral Equation

Integral equations involve an unknown function, $f(x)$ and the integral of $f(x)$. If the unknown function only appears under the integral sign, the integral equation is categorized as the first kind. If the unknown function appears both inside and outside the integral sign, the integral equation is said to be of the second kind.

The Fredholm integral equation of the first kind is

$$f(x) = \int_a^b K(x,t)\phi(t)dt$$

The Fredholm integral equation of the second kind is

$$\phi(x) = f(x) + \int_a^b K(x,t)\phi(t)dt$$

3 Numerical Method: the Modified Galerkin Method

For the more complicated form of the Helmholtz Equation, there is no known closed analytical solution. Therefore, we approached the problem via numerical analysis, specifically, the Modified Galerkin method. Similar to the finite element method, the Galerkin method discretizes the integrating domain into subdomains of different sizes and utilizes a double sum to obtain the final result. The surface integration is of the form (integral over a unit sphere in spherical coordinates)

$$I(f) = \int_U f(q) d\sigma_q = \int_0^{2\pi} \int_0^{\pi} f(\phi, \theta) \sin\theta d\theta d\phi$$

This double integral can be approximated through the Galerkin Method based on the Gaussian Quadrature

$$I_M(f) = \frac{\pi}{M} \sum_{i=1}^{2M} \sum_{j=1}^{M} \omega_j f(\phi_i, \theta_j)$$

where ω_j are the weight functions chosen from the basis $\omega(x) \in \phi_i(x)_{i=1}^n$. [9]

However, the fundamental solution of the Helmholtz Equation, $\frac{e^{ikr_{qA}}}{r_{qA}}$, has a weak singularity at points closer to the boundary. Specifically, r denotes the distance between the point source and the surface of the object. As a result, if the waves originated from a point closer and closer to the object, or in other words, as $r \to 0$, the denominator approaches zero which then creates a weak singularity. To solve that issue, I modified the Galerkin method by adding an infinite series to the fundamental solution to reduce the discontinuity effect. This method is called the Modified Galerkin Method. The series is given by

$$\chi(A, q) = ik \sum_{n=0}^{\infty} \sum_{m=-n}^{n} a_{nm} h_n^{(1)}(k|A|) Y_n^m \left(\frac{A}{|A|}\right) h_n^{(1)}(k|q|) Y_n^m \left(\frac{q}{|q|}\right)$$

where

$$a_{nm} = -\frac{1}{2} \left(\frac{j_n(kR)}{h_n^{(1)}(kR)} + \frac{j_n^{'}(kR)}{h_n^{(1)}(kR)} \right)$$

The basis functions (spherical harmonics) are given by

$$Y_n^m(\phi, \theta) = \left(\frac{1}{2\pi} \left(m + \frac{1}{2} \right) \frac{(m-n)!}{(m+n)!} \right)^{\frac{1}{2}} p_n^m(\cos\theta) e^{\dot{}} im\phi$$

where j_n and $h_n^{(1)}$ are Bessel and Henkel functions of the first kind respectively, and p_n^m is the Legendre function.

3.1 Potential Theory

According to potential theory, the solutions of the Laplace equation are the single layer and double layer potentials [8]. The single layer potential is

$$u(A) = \int_S u(q) \frac{\partial \left(\frac{e^{ikr}}{4\pi r} + \chi(A, q) \right)}{\partial v_q} d\sigma_q$$

While the double layer potential is

$$u(x) = \frac{-1}{4\pi}\int_S \frac{\partial}{\partial v}\frac{1}{|x-y|}d\sigma(y)$$

$$u(x) = 2\pi u(x) + \int_S u(y)\left(\frac{\partial\phi(x,y)}{\partial v} + i\lambda\phi(x,y)\right)d\sigma_y$$

where

$$\phi(x,y) = \frac{e^{-ikr}}{r} - 4\pi\chi(x,y)$$

The solution is given by

$$u(x) = \int v_y \frac{e^{ikr}}{r} + \frac{\partial}{\partial v_y}\left(\frac{e^{ikr}}{r}\lambda + \chi\right)$$

3.2 True Solution of the Helmholtz Equation

Lemma 1:

The following function is the fundamental solution for the Helmholtz equation

$$u = \frac{e^{ikr}}{r^2}(1+\frac{i}{kr})z \quad \text{where } z = \sqrt{x^2+y^2+z^2}$$

Proof:

In order for u to be the solution for the Helmholtz equation, it has to satisfy

$$\Delta u + ku^2 = 0$$

where Δ is the second partial derivatives.

To start with, let's compute the first partial derivatives of u

$$\frac{\partial u}{\partial x} = \frac{ike^{ikr}}{r^3}(1+\frac{i}{kr})zx - \frac{2e^{ikr}}{r^4}(1+\frac{i}{kr})zx - \frac{ie^{ikr}}{r^5k}zx$$

$$\frac{\partial u}{\partial y} = \frac{ike^{ikr}}{r^3}(1+\frac{i}{kr})zy - \frac{2e^{ikr}}{r^4}(1+\frac{i}{kr})zy - \frac{ie^{ikr}}{r^5k}zy$$

$$\frac{\partial u}{\partial z} = \frac{ike^{ikr}}{r^3}(1+\frac{i}{kr})zz - \frac{2e^{ikr}}{r^4}(1+\frac{i}{kr})zz - \frac{ie^{ikr}}{r^5k}zz + \frac{e^{ikr}}{r^2}$$

The next step is to further compute the second partials

$$\frac{\partial^2 u}{\partial x^2} = -\frac{5ike^{ikr}}{r^5}(1+\frac{i}{kr})zx^2 + \frac{ike^{ikr}}{r^3}(1+\frac{i}{kr})z - \frac{k^2e^{ikr}}{r^4}(1+\frac{i}{kr})zx^2 + \frac{2e^{ikr}}{r^6}zx^2 + \frac{8e^{ikr}}{r^6}(1+\frac{i}{kr})zx^2 + \frac{7ie^{ikr}}{kr^7}zx^2 - \frac{2e^{ikr}}{r^4}(1+\frac{i}{kr})z - \frac{ie^{ikr}}{kr^5}z$$

$$\frac{\partial^2 u}{\partial y^2} = -\frac{5ike^{ikr}}{r^5}(1+\frac{i}{kr})zy^2 + \frac{ike^{ikr}}{r^3}(1+\frac{i}{kr})z - \frac{k^2e^{ikr}}{r^4}(1+\frac{i}{kr})zy^2 + \frac{2e^{ikr}}{r^6}zy^2 + \frac{8e^{ikr}}{r^6}(1+\frac{i}{kr})zy^2 + \frac{7ie^{ikr}}{kr^7}zy^2 - \frac{2e^{ikr}}{r^4}(1+\frac{i}{kr})z - \frac{ie^{ikr}}{kr^5}z$$

$$\frac{\partial^2 u}{\partial z^2} = -\frac{5ike^{ikr}}{r^5}(1+\frac{i}{kr})zz^2 + \frac{3ike^{ikr}}{r^3}(1+\frac{i}{kr})z - \frac{k^2e^{ikr}}{r^4}(1+\frac{i}{kr})zz^2 + \frac{2e^{ikr}}{r^6}zz^2 + \frac{8e^{ikr}}{r^6}(1+\frac{i}{kr})zz^2 + \frac{7ie^{ikr}}{kr^7}zz^2 - \frac{6e^{ikr}}{r^4}(1+\frac{i}{kr})z - \frac{3ie^{ikr}}{kr^5}z$$

Summing the three second partials, we obtain

$$\Delta u = -\frac{5ike^{ikr}}{r^5}(1+\frac{i}{kr})zr^2 + \frac{5ike^{ikr}}{r^3}(1+\frac{i}{kr})z - \frac{k^2e^{ikr}}{r^4}(1+\frac{i}{kr})zr^2 + \frac{2e^{ikr}}{r^6}zr^2 \frac{8e^{ikr}}{r^6}(1+\frac{i}{kr})zr^2 + \frac{7ie^{ikr}}{kr^7}zr^2 - \frac{10e^{ikr}}{r^4}(1+\frac{i}{kr})z - \frac{5ie^{ikr}}{kr^5}z$$

because of the fact that $r^2 = x^2 + y^2 + z^2$

To complete the Helmholtz equation, the last term k^2u is added to the previous sum

$$\begin{aligned}
\Delta u + k^2 u =& -\frac{5ike^{ikr}}{r^5}(1+\frac{i}{kr})zr^2 + \frac{5ike^{ikr}}{r^3}(1+\frac{i}{kr})z - \frac{k^2e^{ikr}}{r^4}(1+\frac{i}{kr})zr^2 + \frac{2e^{ikr}}{r^6}zr^2 + ... \\
& \frac{8e^{ikr}}{r^6}(1+\frac{i}{kr})zr^2 + \frac{7ie^{ikr}}{kr^7}zr^2 - \frac{10e^{ikr}}{r^4}(1+\frac{i}{kr})z - \frac{5ie^{ikr}}{kr^5}z + \frac{k^2e^{ikr}}{r^2}(1+\frac{i}{kr})z \\
\Delta u + k^2 u =& -\frac{5ike^{ikr}}{r^3}(1+\frac{i}{kr})z + \frac{5ike^{ikr}}{r^3}(1+\frac{i}{kr})z - \frac{k^2e^{ikr}}{r^2}(1+\frac{i}{kr})z + \frac{2e^{ikr}}{r^4}z + ... \\
& \frac{8e^{ikr}}{r^4}(1+\frac{i}{kr})z + \frac{7ie^{ikr}}{kr^5}z - \frac{10e^{ikr}}{r^4}(1+\frac{i}{kr})z - \frac{5ie^{ikr}}{kr^5}z + \frac{k^2e^{ikr}}{r^2}(1+\frac{i}{kr})z \\
\Delta u + k^2 u =& \frac{2e^{ikr}}{r^4}z + \frac{2e^{ikr}}{kr^5}iz - \frac{2e^{ikr}}{r^4}(1+\frac{i}{kr})z \\
=& \frac{2e^{ikr}}{r^4}z + \frac{2e^{ikr}}{kr^5}iz - \frac{2e^{ikr}}{r^4}z - \frac{2e^{ikr}}{kr^5}iz \\
=& 0
\end{aligned}$$

This shows that u satisfies the Helmholtz equation. It is therefore the fundamental solution.[]

3.3 Hankel and Bessel functions

The Bessel function of the first kind, $J_n(z)$ is given by

$$J_n(z) = \frac{1}{2\pi i}\int e^{(z/2)(t-1/t)}t^{-n-1}dt$$

Then the Bessel function of the second kind, $Y_v(z)$ is given by

$$Y_v(z) = \frac{J_v(z)\cos(v\pi) - J_{-v}(z)}{\sin(v\pi)}$$

While the Hankel function of the first kind [8], $H_n^{(1)}$ is given by

$$H_n^{(1)} = J_n(z) + iY_n(z)$$

3.4 LU Decomposition

LU Decomposition is a method for breaking down a given matrix into product of the upper and lower triangular matrices. The primary purpose for this method is to solve linear systems of the kind $Ax = b$, where A is the coefficient matrix, x is the vector of variables, b is the augmented vector. LU Decomposition depends only on the matrix A without any operation on b. In fact, any value of b can be solved once A is completely decomposed. Therefore, it is an advantage for using this method in computer computations involving solving systems of equations that have different b values, which occurs often in testing multiple physical and real-life problems.

4 Integrating Martian atmospheric properties

For the more realistic impedance problem, the assumption of total reflection or absorption is not applicable since this would require an idealized object in both shape and material rather than a real one. Therefore, a combination of partial reflection and partial absorption is expected. The ratio of these two responses depends on the physical aspects of the object and the characteristics of the incoming wave. Different kinds of materials result in different reflection ratios. Without the access to a simulated testing environment, I could not determine the exact value for typical materials such as carbon fiber and steel. The reflection ratio is therefore extrapolated from how those materials react with sound waves .

Wavenumbers, also known as spatial frequencies, are physical properties of a wave indicating the number of wave cycles in a specified distance. Frequently, wavenumbers denote angular wavenumbers that have a unit of radians over distance. The calculation of wavenumbers is related to the wavelength by

$$k = \frac{2\pi}{\lambda},$$

where k is the wavenumber and λ is the wavelength. Since waves span over a variety of range of wavelengths, there is no literature values for wavelength, frequency or velocity of Martian atmospheric pressure wave. A deduction of wavenumber from the most basic properties of atmosphere: pressure and density was performed. We can only use the frequency and velocity as a function of atmospheric pressure and density to deduce the wavenumber.

Altitude (km)	Low Solar Activity		Mean Solar Activity		Extremely High Solar Activity	
	Density (kg/m^3)	Pressure (Pa)	Density (kg/m^3)	Pressure (Pa)	Density (kg/m^3)	Pressure (Pa)
0	1.17E+00	1.01E+05	1.17E+00	1.01E+05	1.16E+00	9.98E+04
20	9.48E-02	5.62E+03	9.49E-02	5.62E+03	9.41E-02	5.57E+03
40	4.07E-03	3.01E+02	4.07E-03	3.02E+02	4.04E-03	2.99E+02
60	3.31E-04	2.32E+01	3.31E-04	2.32E+01	3.28E-04	2.30E+01
80	1.69E-05	9.81E-01	1.68E-05	9.45E-01	1.68E-05	8.42E-01
100	5.77E-07	2.89E-02	5.08E-07	2.81E-02	2.78E-07	2.63E-02
120	1.70E-08	1.92E-03	1.80E-08	2.17E-03	2.34E-08	3.55E-03
140	2.96E-09	5.37E-04	3.26E-09	7.03E-04	4.93E-09	1.61E-03
160	9.65E-10	2.13E-04	1.18E-09	3.31E-04	2.23E-09	9.90E-04
180	3.90E-10	9.62E-05	5.51E-10	1.80E-04	1.28E-09	6.76E-04
200	1.75E-10	4.70E-05	2.91E-10	1.05E-04	8.28E-10	4.86E-04

From the table above [1], I obtained the wave velocity from

$$v = \sqrt{\gamma \frac{P}{\rho}}$$

where γ is the adiabatic index, P the atmospheric pressure and ρ the atmospheric density.

I further constructed the relationship between wave number with pressure and density by utilizing the formula

$$v = \lambda f$$

From this equation, I concluded that

$$k = 2\pi f \sqrt{\frac{\rho}{\gamma P}}$$

Since the Galerkin method produces best results for small wavenumber, I limited the k values to be within $[10^{-5}, 1]$. To justify the assumption, I calculated the corresponding wave frequency at different atmospheric layers. The frequencies fall in the range of [0.4, 250]Hz which are classified as low to extremely low frequency waves.

[1] "Properties of Standard Atmosphere." Rocket and Space Technology, http://www.braeunig.us/space/atmos.htmg

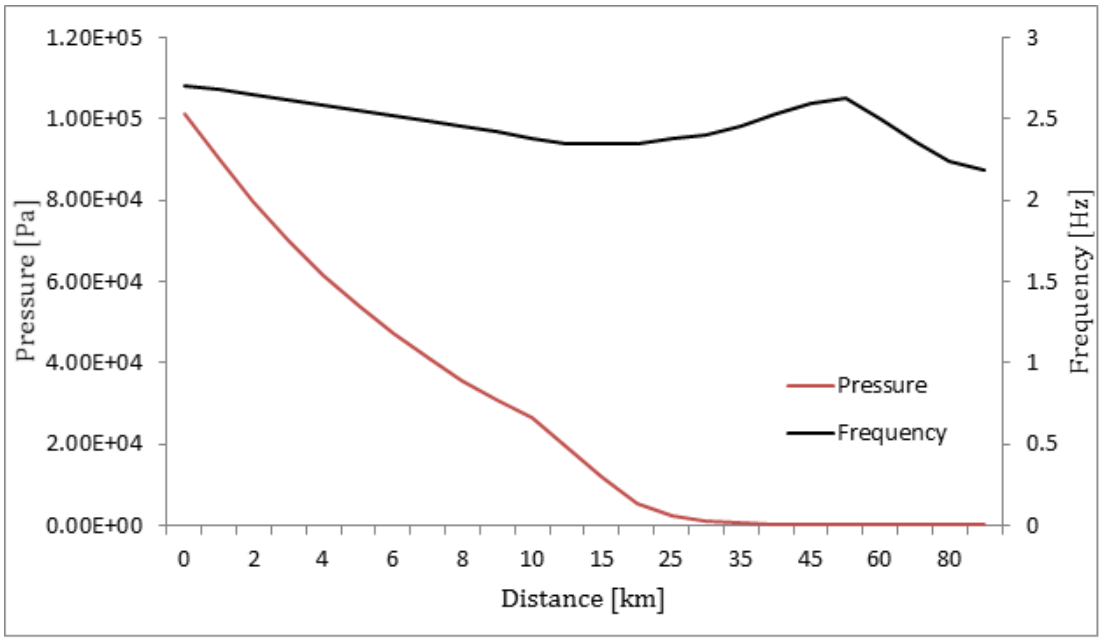

Figure 2: Calculated frequency values for on atmospheric conditions

The figure above shows the correlation between the calculated frequency and atmospheric pressure as functions of distance above the planetary surface. The consistently low frequencies verify the assumption of low wavenumber.

5 Numerical Results

Numerical computations were programmed using Fortran 77 and all calculation was computed in the computer lab MNS 201 at Roger Williams University. I obtained the subroutines from the Naval Surface Warfare Center of Newport, RI.

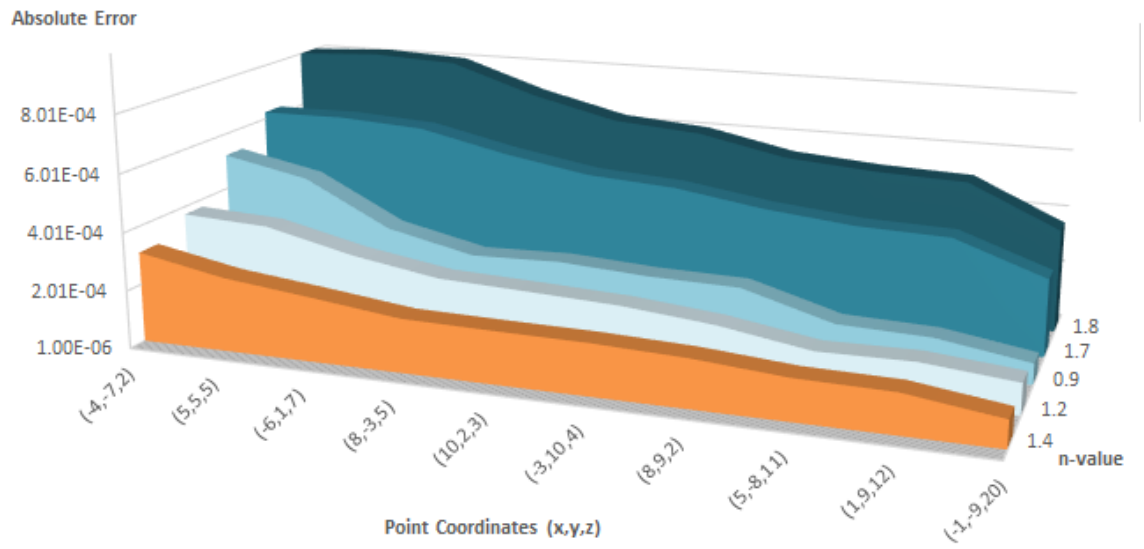

Figure 3: Convergence results for different n-value

Since the coefficients given by Kleinman and Roach are specifically for spheres and spherical regions, I obtained better convergence results only for spherical shapes. However, since the analysis for most spherical shapes were already conducted by Dr. Y. Warnapala, I focused on the shapes that are not exactly spherical. Based on the formula of the superellipsoid, this required values of n that differ than 2.5. For n = 1.4, I obtained the best convergence results and the corresponding shape is smooth and simply connected.

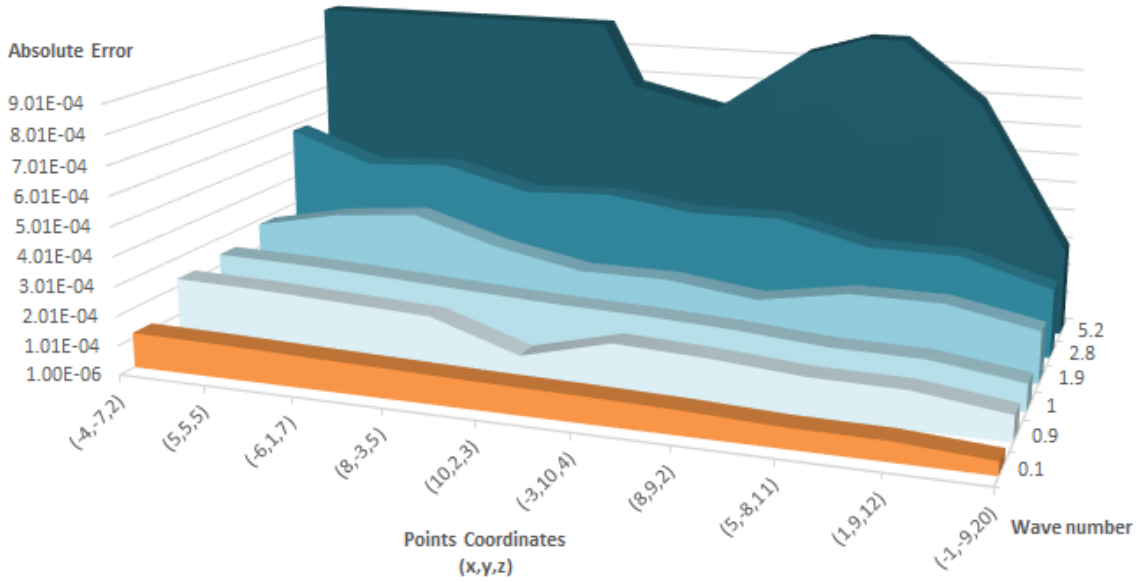

Figure 4: Convergence results for different wavenumber

The numerical applications for the Helmholtz Equation is known to give good results for low wave numbers. I also came to the conclusion that as the wave number increases, the results diverge from the fundamental solution. However, in reality, many waves tend to have high energy and therefore, a high wave number. Thus far, I investigated mainly the largest possible k that produces uniformly convergent values, which is k = 1.

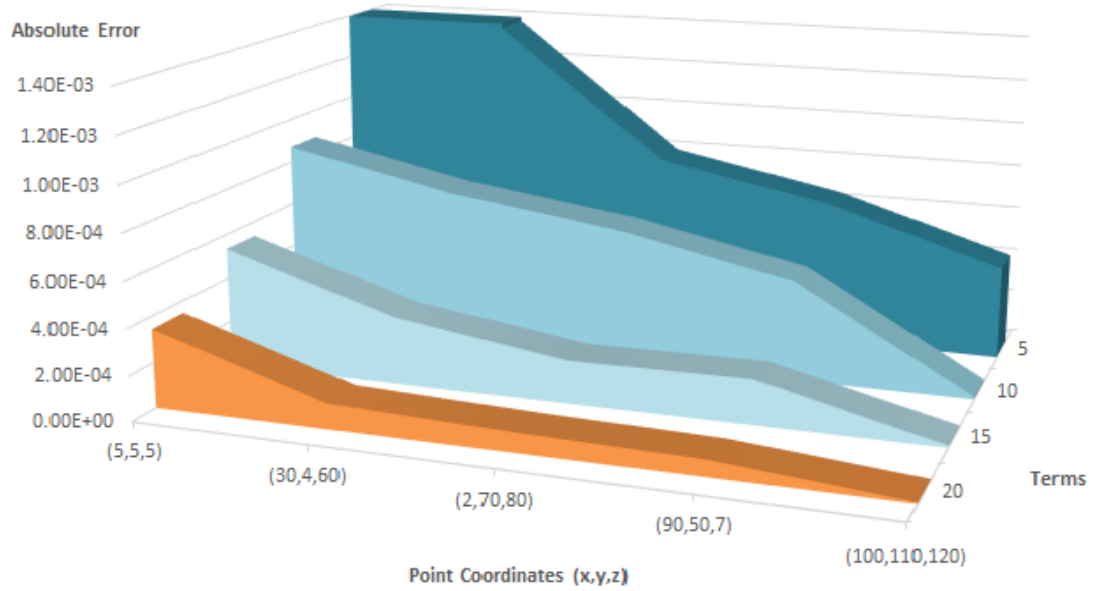

Figure 5: Convergence results for increasing number of terms

From the above analysis, I predicted that the convergence will get better when more terms are added from the infinite series. Because of the limited computer power, I could not add more than 20 terms from the series. For 5 terms, the computing time was less than a minute. However, as more terms were added to the series, it required more processing power as the iterations were multiplied by several times. At 15 terms, it took over an hour to finish the calculation. If different combinations of exterior/interior nodes and high number of terms such as 20 were to execute at the same time, the result could only be obtained after more than a day of continuous running.

6 Final Remarks and Future Work

From the results above, I observed a trend of convergence for the superellipsoid shapes. The results for different wave numbers indicates that as k got larger and larger, the results diverged from the fundamental solution. At this time, I only considered small values of k. Furthermore, as predicted from the method, the convergence became better as more terms were add. This behavior agrees with the hypothesis that the infinite series reduce the effect of the singularity at extremely close distance to the tested object.

My future goal is to modify the superellipsoid to generate a more realistic shape that can be a candidate for the fuselage component design of a space craft. I am considering the idea of stretching the shape along the y-direction and the possibility of developing a model for part of a spacecraft that one day might go to planet Mars.

7 Acknowledgements

I would like to extend special thanks toward Dr. Scott D. Rutherford and Mrs. Patricia Kennedy for their technical support regarding Fortran 77 and formatting the thesis. It was a great experience learning new coding languages and the Unix platform.

I would like to thank EPSCoR Grant, EPSCoR Marine Center Coordinator Jim Lemire, the Rhode Island NASA Space Grant, the Naval Surface Warfar Center of Newport, the Roger Williams University Provost Fund and Math Department for funding this project. The resources supported my work during the semester breaks and allowed me to attend conferences.

I would like to thanks my committee members, Professor Earl Gladue and Dr. Ruth Koelle, for their help on mathematical concepts.

I am grateful for the physical and emotional support from my family and friends during the course of completing this thesis.

I would like to express the deepest appreciation toward my advisor, mentor, and professor, Dr. Yajni Warnapala. Without her guidance, I would not have had the opportunity to explore the entirely new experience of doing scholarly work, and thus this thesis would not have been possible.

References

[1] Abramowitz, Milton, and Irene A. Stegun. *Handbook of Mathematical Functions, National Bureau of Standards*. New York: Dover, 1965. Print

[2] Colton, David L., and Rainer Kress. *Integral Equation Methods in Scattering Theory*. New York: Wiley, 1983. Print.

[3] "Émile Léonard Mathieu*." Mathieu_Emile Biography, history.mcs.st-andrews.ac.uk*.Web. 2014.

[4] Jenkins, Gwilym M., and Donald G. Watts. Spectral Analysis and Its Applications. San Francisco: Holden-Day, 1968. Print.

[5] Kahn, Michael N. Technical Analysis Plain and Simple: Charting the Markets in Your Language. 3rd ed. Upper Saddle River, NJ: Financial Times Prentice Hall, 2006. Print.

[6] Lay, Steven R. *Analysis: With an Introduction to Proof*. 2nd ed. Englewood Cliffs, NJ: Prentice Hall, 1990. Print.

[7] The Editors of Encyclopædia Britannica. "Rudolf Friedrich Alfred Clebsch (German Mathematician)." Encyclopedia Britannica Online. Encyclopedia Britannica, Web. 2014.

[8] Y. Warnapala, and Morgan E. " The Numerical Solution of the Exterior Dirichlet Problem for the Helmholtz's Equation via Modified Green's functions approach for the Oval of Cassini." *Computers & Math. w. Applic* (2004): Print.

[9] Y. Warnapala, and Hy D. "The Numerical Solution of the Helmholtz's Equation for the Superellipsoid via the Galerkin Mathod for the Dirichlet Problem" *Communications in Numerical Analysis* (2004): Print.

[10] Y. Warnapala., Pleskunas, J. and Siegel, R. "The Numerical Solution of the Exterior Boundary Value Problems for the Helmholtz's Equation for the Pseudosphere." *IAENG International Journal of Applied Mathematics 41* (2011): Print

[11] Y. Warnapala, and Yehiya. "The Numerical Solution of Exterior Robin Problem for the Helmholtz's Equation via Modified Integral Equation Approach." *Far East Journal of Applied Mathematics* (2005): n. Print.

[12] Y. Warnapala, and Yehiya. "The Numerical solution of exterior Neumann problem for Helmholtz's equation via modified Green's functions approach." *Far East Journal of Applied Mathematics* (2004): n. Print.

[13] Yogi Ahmad, ERLANGGA. "A Robust and Ecien T Iterativ E Metho D for the N Umerical Solution of the Helmholtz Equation." Web. 2014.

Appendix A: Tables and Graphs

Altitude (km)	Low Solar Activity		Mean Solar Activity		Extremely High Solar Activity	
	Density (kg/m^3)	Pressure (Pa)	Density (kg/m^3)	Pressure (Pa)	Density (kg/m^3)	Pressure (Pa)
0	1.17E+00	1.01E+05	1.17E+00	1.01E+05	1.16E+00	9.98E+04
20	9.48E-02	5.62E+03	9.49E-02	5.62E+03	9.41E-02	5.57E+03
40	4.07E-03	3.01E+02	4.07E-03	3.02E+02	4.04E-03	2.99E+02
60	3.31E-04	2.32E+01	3.31E-04	2.32E+01	3.28E-04	2.30E+01
80	1.69E-05	9.81E-01	1.68E-05	9.45E-01	1.68E-05	8.42E-01
100	5.77E-07	2.89E-02	5.08E-07	2.81E-02	2.78E-07	2.63E-02
120	1.70E-08	1.92E-03	1.80E-08	2.17E-03	2.34E-08	3.55E-03
140	2.96E-09	5.37E-04	3.26E-09	7.03E-04	4.93E-09	1.61E-03
160	9.65E-10	2.13E-04	1.18E-09	3.31E-04	2.23E-09	9.90E-04
180	3.90E-10	9.62E-05	5.51E-10	1.80E-04	1.28E-09	6.76E-04
200	1.75E-10	4.70E-05	2.91E-10	1.05E-04	8.28E-10	4.86E-04

Table 1: Atmospheric data of Earth

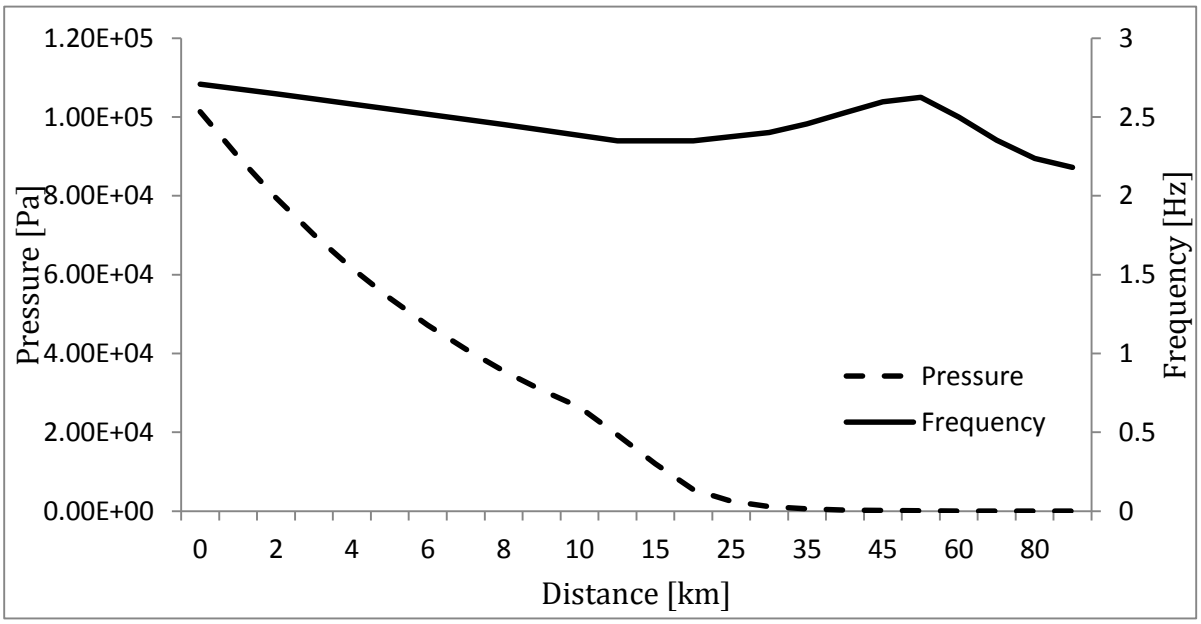

Figure 1: Plot of wave frequency (obtained from atmospheric pressure and density) and atmospheric pressure vs. distance from Martian surface.

External points from which the waves originate						
k values	0.05	0.052278	0.065348	0.078417	0.091487	0.01
(80,90,100)	1.44E-05	1.40E-05	1.31E-05	1.59E-05	2.28E-05	2.06E-05
(500,2,5)	4.56E-06	4.43E-06	4.02E-06	4.69E-06	6.58E-06	6.46E-06
(2,500,5)	5.56E-06	4.43E-06	4.02E-06	4.69E-06	6.58E-06	6.46E-06
(2,5,500)	4.41E-06	4.30E-06	4.19E-06	5.43E-06	7.92E-06	6.45E-06
(300,400,500)	3.17E-06	3.09E-06	2.89E-06	3.56E-06	5.11E-06	4.56E-06

Table 2: Absolute errors of different wavenumbers with varying distances from the tested object

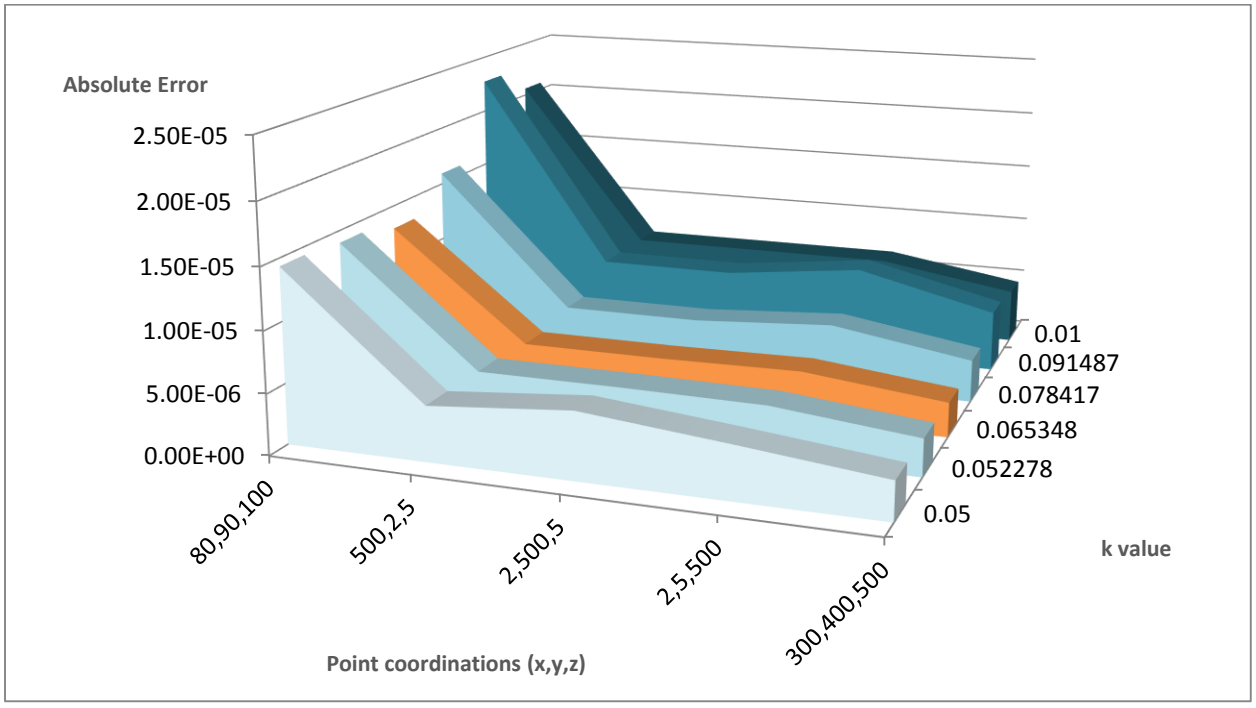

Figure 2: Absolute errors of different wavenumbers with varying distances from the tested object

Superellipsoid shapes ranging from 0.9 to 1.8					
n-values	1.4	1.2	0.9	1.7	1.8
(-4,-7,2)	3.12E-04	3.74E-04	5.23E-04	6.27E-04	8.03E-04
(5,5,5)	2.55E-04	3.59E-04	4.63E-04	6.29E-04	8.18E-04
(-6,1,7)	2.22E-04	2.88E-04	3.09E-04	6.10E-04	8.03E-04
(8,-3,5)	1.85E-04	2.39E-04	2.41E-04	5.43E-04	7.03E-04
(10,2,3)	1.80E-04	2.26E-04	2.49E-04	4.91E-04	6.29E-04
(-3,10,4)	1.77E-04	2.12E-04	2.30E-04	4.70E-04	6.04E-04
(8,9,2)	1.66E-04	1.83E-04	2.24E-04	4.23E-04	5.40E-04
(5,-8,11)	1.41E-04	1.32E-04	1.34E-04	3.91E-04	5.16E-04
(1,9,12)	1.36E-04	1.36E-04	1.23E-04	3.81E-04	5.04E-04
(-1,-9,20)	9.34E-05	1.07E-04	7.37E-05	2.70E-04	3.61E-04

Table 3: Varying shapes of superellipsoids from n = [0.5, 1.8]

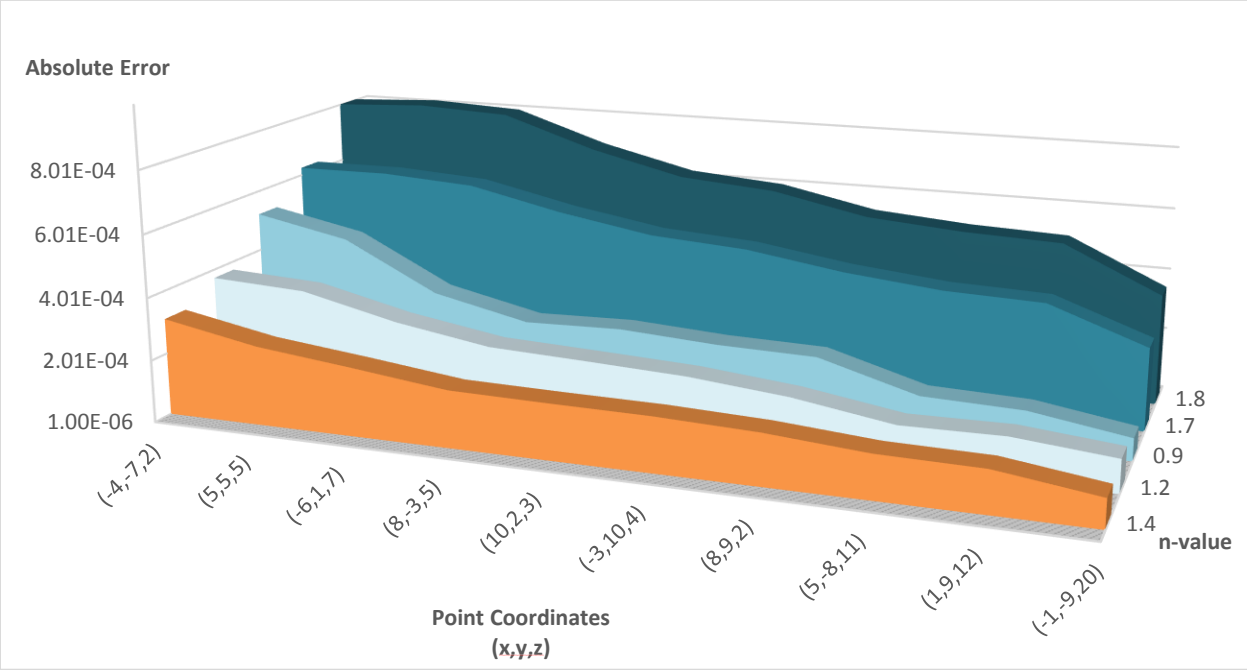

Figure 3: Varying shapes of superellipsoids from n = [0.5, 1.8]

Absolute Errors for different wavenumbers						
k values	0.1	0.9	1	1.9	2.8	5.2
(-4,-7,2)	1.20E-04	2.29E-04	2.42E-04	2.84E-04	5.81E-04	1.08E-03
(5,5,5)	1.15E-04	2.21E-04	2.35E-04	3.46E-04	4.77E-04	1.91E-03
(-6,1,7)	1.08E-04	2.08E-04	2.22E-04	3.74E-04	4.95E-04	1.64E-03
(8,-3,5)	1.01E-04	1.93E-04	2.05E-04	2.86E-04	4.20E-04	1.36E-03
(10,2,3)	9.36E-05	9.44E-05	1.90E-04	2.28E-04	4.37E-04	7.83E-04
(-3,10,4)	8.90E-05	1.71E-04	1.81E-04	2.27E-04	3.96E-04	7.18E-04
(8,9,2)	8.15E-05	1.57E-04	1.66E-04	1.88E-04	4.01E-04	9.34E-04
(5,-8,11)	6.88E-05	1.32E-04	1.41E-04	2.40E-04	3.28E-04	1.03E-03
(1,9,12)	6.63E-05	1.28E-04	1.36E-04	2.39E-04	3.26E-04	7.97E-04
(-1,-9,20)	4.54E-05	8.71E-05	9.34E-05	1.78E-04	2.39E-04	2.98E-04

Table 4: Comparison between different wave numbers from 0.1 to 5.2

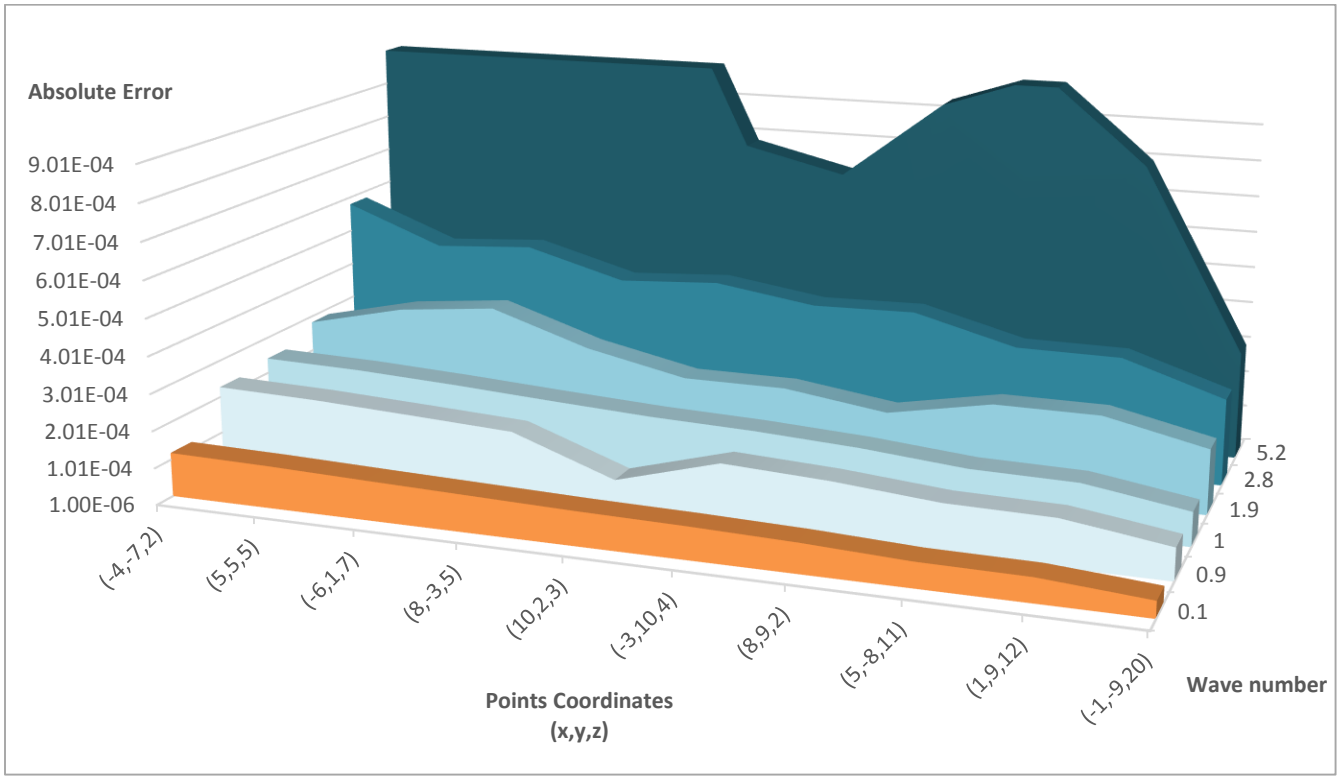

Figure 4: Comparison between different wave numbers from 0.1 to 5.2

Absolute errors for finite numbers of terms from the infinite series				
# of Terms	20	15	10	5
(5,5,5)	3.45E-04	5.35E-04	8.71E-04	8.96E-03
(30,4,60)	1.11E-04	3.02E-04	7.14E-04	1.38E-03
(2,70,80)	8.62E-05	1.91E-04	6.08E-04	8.00E-04
(90,50,7)	7.10E-05	1.98E-04	4.49E-04	6.51E-04
-100,110,120	6.66E-06	1.06E-05	1.20E-05	4.16E-04

Table 5: Number of terms added from the infinite series

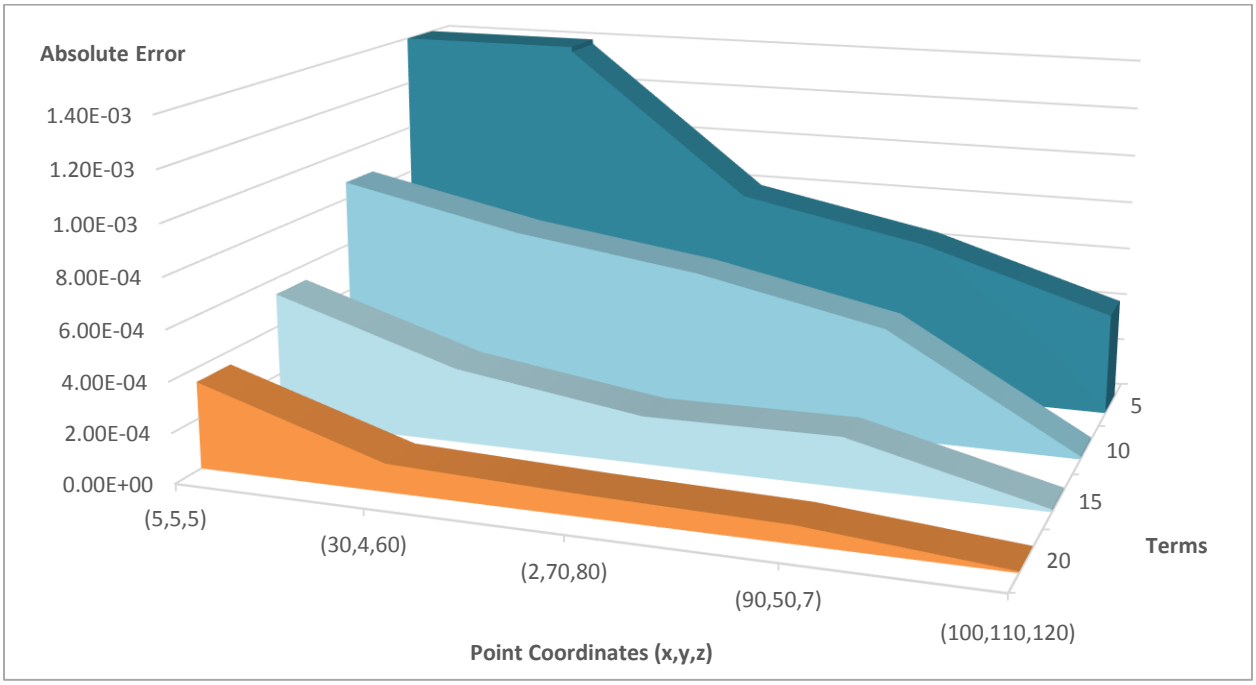

Figure 5: Number of terms added from the infinite series

Different wavenumbers obtained from extrapolated Martian atmospheric data						
Density [kg/m3]	Pressure [Pa]	Velocity [m/s]	Frequency [Hz]			
			4	5	6	7
6.52E-11	5.624E-06	347.50645	0.0723231	0.0904039	0.1084846	0.1265654
2.36E-11	2.648E-06	396.33918	0.0634122	0.0792653	0.0951183	0.1109714
1.102E-11	1.44E-06	427.71499	0.0587605	0.0734506	0.0881407	0.1028309
5.82E-12	8.4E-07	449.51291	0.0559111	0.0698888	0.0838666	0.0978443
3.32E-12	5.152E-07	466.10408	0.0539209	0.0674011	0.0808813	0.0943615
1.982E-12	3.272E-07	480.74950	0.0522782	0.0653478	0.0784174	0.0914869
1.232E-12	2.128E-07	491.75012	0.0511088	0.0638860	0.0766631	0.0894403
7.88E-13	1.416E-07	501.57114	0.0501008	0.0626350	0.0751625	0.0876891
5.16E-13	9.6E-08	510.35783	0.0492453	0.0615567	0.0738683	0.0861793
3.44E-13	6.56E-08	516.69792	0.0486411	0.0608013	0.0729616	0.0851219
2.32E-13	4.552E-08	524.10844	0.0479533	0.0599417	0.0719301	0.0839183
1.598E-13	3.184E-08	528.15593	0.0475858	0.0594823	0.0713788	0.0832752

Table 6: Table of wavenumber from predetermined frequency

Appendix B*

1. Bessel functions of the first kind

Bessel functions of the first kind, denoted as Jα(x), are solutions of Bessel's differential equation that are finite at the origin (x = 0) for integer or positive α, and diverge as x approaches zero for negative non-integer α. It is possible to define the function by its Taylor series expansion around x = 0, which can be found by applying the Frobenius method to Bessel's equation:

$$J_\alpha(x) = \sum_{m=0}^{\infty} \frac{(-1)^m}{m!\,\Gamma(m+\alpha+1)} \left(\frac{x}{2}\right)^{2m+\alpha}$$

where Γ(z) is the gamma function, a shifted generalization of the factorial function to non-integer values. The Bessel function of the first kind is an entire function if α is an integer, otherwise it is a multivalued function with singularity at zero.

2. Galerkin Method

A method of determining coefficients α_k in a power series solution

$$y\,(x) = y_0\,(x) + \sum_{k=1}^{n} \alpha_k\, y_k\,(x)$$

of the ordinary differential equation $\tilde{L}[y(x)] = 0$ so that $\tilde{L}[y(x)]$, the result of applying the ordinary differential operator to y(x), is orthogonal to every $y_k(x)$ for k=1, ..., n (Itô 1980).

Galerkin methods are equally ubiquitous in the solution of partial differential equations, and in fact form the basis for the finite element method.

3. Simply Connected

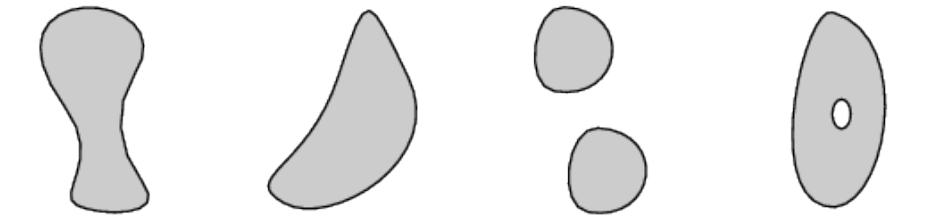

simply connected *simply connected* *not simply connected* *not simply connected*

A pathwise-connected domain is said to be simply connected (also called 1-connected) if any simple closed curve can be shrunk to a point continuously in the set. If the domain is connected but not simply, it is said to be multiply connected. In particular, a bounded subset E of R^2 is said to be simply connected if both E and R^2\E, where F\E denotes a set difference, are connected.

A space S is simply connected if it is pathwise-connected and if every map from the 1-sphere to S extends continuously to a map from the 2-disk. In other words, every loop in the space is contractible.

* This appendix provides additional techical concepts which are directly obtained from various mathematical online libraries such as WolframAlpha, Mathisfun and other math resources.

4. Laplace's equation

The scalar form of Laplace's equation is the partial differential equation

$$\nabla^2\psi = 0$$

where ∇^2 is the Laplacian.

Note that the operator ∇^2 is commonly written as Δ by mathematicians (Krantz 1999, p. 16). Laplace's equation is a special case of the Helmholtz differential equation

$$\nabla^2\psi + k^2\psi = 0 \qquad \text{with k=0}$$

A function ψ which satisfies Laplace's equation is said to be harmonic. A solution to Laplace's equation has the property that the average value over a spherical surface is equal to the value at the center of the sphere (Gauss's harmonic function theorem). Solutions have no local maxima or minima. Because Laplace's equation is linear, the superposition of any two solutions is also a solution.

5. Helmholtz Resonance

Helmholtz resonance is the phenomenon of air resonance in a cavity, such as when one blows across the top of an empty bottle. The name comes from a device created in the 1850s by Hermann von Helmholtz, the "Helmholtz resonator", which he, the author of the classic study of acoustic science, used to identify the various frequencies or musical pitches present in music and other complex sounds.

$$\omega_H = \sqrt{\gamma \frac{A^2}{m} \frac{P_0}{V_0}}$$

where:

γ is the adiabatic index or ratio of specific heats. This value is usually 1.4 for air and diatomic gases.

A is the cross-sectional area of the neck;

m is the mass in the neck;

P_0 is the static pressure in the cavity;

V_0 is the static volume of the cavity.

6. Drag Coefficient

In fluid dynamics, the drag coefficient is a dimensionless quantity that is used to quantify the drag or resistance of an object in a fluid environment, such as air or water. It is used in the drag equation, where a lower drag coefficient indicates the object will have less aerodynamic or hydrodynamic drag. The drag coefficient is always associated with a particular surface area.

The drag coefficient c_d is defined as:

$$c_d = \frac{2F_d}{\rho v^2 A}$$

where:

F_d is the drag force, which is by definition the force component in the direction of the flow velocity,[6]

ρ is the mass density of the fluid,[7]

v is the speed of the object relative to the fluid,

A is the reference area.

7. Gauss Quadrature

In numerical analysis, a quadrature rule is an approximation of the definite integral of a function, usually stated as a weighted sum of function values at specified points within the domain of integration. An n-point Gaussian quadrature rule, named after Carl Friedrich Gauss, is a quadrature rule constructed to yield an exact result for polynomials of degree 2n − 1 or less by a suitable choice of the points xi and weights w_i for i = 1, ..., n. The domain of integration for such a rule is conventionally taken as [−1, 1], so the rule is stated as

$$\int_{-1}^{1} f(x)\,dx \approx \sum_{i=1}^{n} w_i f(x_i).$$

Some low-order rules for solving the integration problem are listed below.

Number of points, *n*	**Points, x_i**	**Weights, w_i**
1	0	2
2	$\pm\sqrt{\frac{1}{3}}$	1
3	0	$\frac{8}{9}$
	$\pm\sqrt{\frac{3}{5}}$	$\frac{5}{9}$
4	$\pm\sqrt{\frac{3}{7}-\frac{2}{7}\sqrt{\frac{6}{5}}}$	$\frac{18+\sqrt{30}}{36}$
	$\pm\sqrt{\frac{3}{7}+\frac{2}{7}\sqrt{\frac{6}{5}}}$	$\frac{18-\sqrt{30}}{36}$
5	0	$\frac{128}{225}$
	$\pm\frac{1}{3}\sqrt{5-2\sqrt{\frac{10}{7}}}$	$\frac{322+13\sqrt{70}}{900}$
	$\pm\frac{1}{3}\sqrt{5+2\sqrt{\frac{10}{7}}}$	$\frac{322-13\sqrt{70}}{900}$

The thesis of *Hy Dinh* was reviewed and approved by the following:

_____ Date _____
Dr. Yajni Warnapala
Thesis advisor

_____ Date _____
Dr. Ruth Koelle
Thesis committee member

_____ Date _____
Prof. Earl Gladue
Thesis committee member